Estimation of unknown stiffness using electromagnetic force balance and virtual input shaping for uncertainty calculation

Sylvain Hernandez[1,*], Joël Abadie[1], Eric Lesniewska[2], Emmanuel Piat[1]

***Abstract*— Small force measurements are needed in a large variety of cutting-edge scientific applications. However, the development of small-scale force standards and suitable calibration procedures remains challenging for national institutes of metrology. In this context, an electromagnetic force balance is under development to characterize flexible samples or calibrate force transducers down to the micronewton level. The main contribution of this work is the application to this system of a methodological proposal in order to estimate the stiffness of a flexible cantilever. This method consists of four distinct steps based on the existing concept of equivalent representation for uncertain dynamical systems. The calculation of uncertainty for specific quantities of interest, such as stiffness, is therefore linked to this concept using interval analysis and unknown input shaping.**

***Index Terms*— Small force metrology, Stiffness estimation, Unknown input, Uncertainty calculation, Interval analysis.**

I. Introduction

According to the database (KCDB) of the mutual recognition agreement of National Metrology Institutes (NMIs), the traceability of small force measurements cannot be guaranteed below 0.1 N at the international level. However, a large panel of scientific applications involves much smaller forces, possibly down to the attonewton (10^{-18} N) [1], whereas the measuring instruments used do not benefit from an appropriate calibration procedure, as there is no small force standard at this scale.

Therefore, NMIs and research laboratories put a lot of efforts in the development of reference standards and transfer artefacts to disseminate the force unit [2], and lend more credibility to the scientific activities concerned. An electromagnetic small force generator has been developed to apply microforces on rigid samples [3], which is inspired of deadweight machines that are traditionally used at macroscale to produce force standards. Indeed, the weight of a levitating magnetic indenter subjected to the effect of the local gravitational field is applied on the sample. The redefinition of the kilogram unit using electrical metrology units motivated NMIs to design electrostatic force balances [4], which currently represent a promising approach to produce small force standards. Consequently, the above-mentioned force generator is currently being converted into an electromagnetic force balance, with a similar operating principle based on the regulation of the indenter levitation height. As stiffness references are widespread and useful transfer artifacts, this new device aims to characterize the spring constant of flexible cantilevers in bending using the indenter tip. The electromagnetic force balance is therefore a dynamical system, coupled with the cantilever of unknown stiffness to be characterized.

In the field of dynamic measurements, calculating uncertainty in accordance with the guidelines of the Guide to the expression of Uncertainty in Measurement (GUM) remains a challenge for dynamical systems [5], that could be tackled using control theory tools [6]. From the force balance point of view, the force applied by the cantilever, but also all the external disturbances and model discrepancies correspond to unknown inputs that make the force balance uncertain. In Reference [7], an exact manner of representing the true behavior of a specific class of uncertain dynamical SISO systems is presented, but the calculation of uncertainty is not addressed. This work builds on this concept of equivalent representation to extend it, and thus propose a new methodology for determining the measurement uncertainty of the electromagnetic force balance.

II. Presentation of the system

Fig. 1a illustrates the early prototype of the force balance studied in this paper, and whose typical range is between 10^{-4} N.m^{-1} and 1 N.m^{-1}. The levitating indenter is made of a thin capillary glass tube to the end of which is fixed a small cylindrical magnet of 1×1 mm. The levitation is guaranteed by a constant electromagnetic force produced by coils, combined with stabilizing diamagnetic forces generated by graphite plates surrounding the small magnet. The electrical current is generated by a KIKUSUI DC Power supply PBZ40-10, and the levitation height is measured using a chromatic confocal sensor PRECITEC CHRocodile S. The nonmagnetic cantilever to be characterized is a 0.1mm-thin flexible plastic film mounted at one end on a PI micromanipulator, in order to be moved. While the other free end of the cantilever is pushed against the indenter, the implemented control law adjusts the current injected into the coils to keep the indenter at its initial levitation height, thus causing the cantilever to bend. The resulting deformation is measured and used to estimate its stiffness.

A. Mechanical modeling

The modeling of the electromagnetic force balance has already been presented in detail in [3], and is therefore briefly

*Corresponding author: sylvain.hernandezsabio@gmail.com;
[1]Department of Automatic Control and Micro-Mechatronic Systems, FEMTO-ST Institute, CNRS UMR 6174, University Bourgogne Franche-Comté, 24 rue Alain Savary, 25000 Besançon, France;
[2]Department of Nanosciences, ICB, CNRS UMR 6303, University Bourgogne Franche Comté, 9 Av. Savary, 21078 Dijon, France.

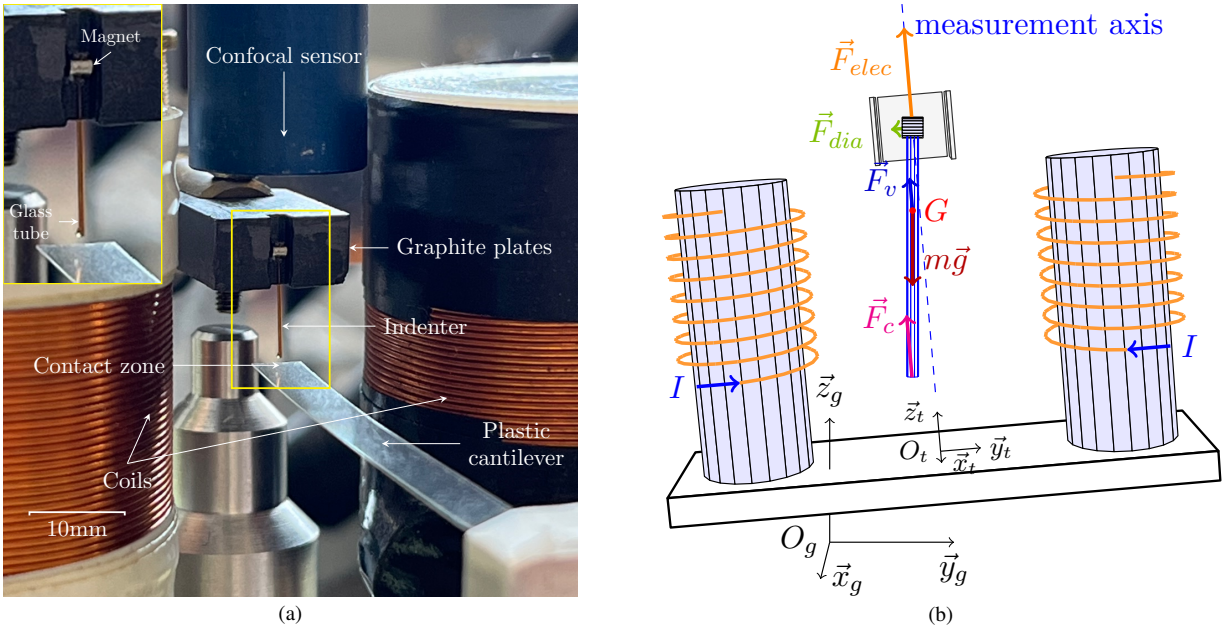

(a) (b)

Fig. 1. (a) Picture of the electromagnetic force balance prototype. (b) Schematic representation used for modeling.

recalled here with some adjustments. The schematic representation used to carry out the mechanical modeling is shown in Fig. 1b. The setup is mounted on a vibration isolation table associated with a moving frame $R_t = (O_t, \vec{x}_t, \vec{y}_t, \vec{z}_t)$, defined in relation to the inertial frame $R_g = (O_g, \vec{x}_g, \vec{y}_g, \vec{z}_g)$ linked to the laboratory. Nevertheless, the inclination of the table varies slowly, which disturbs the dynamic behavior of the force balance. The angles α_x, α_y are introduced to describe the orientation of R_t with respect to R_g. Noting by m the mass of the levitating indenter, its weight $\vec{W}$ is expressed in R_t as follows:

$$\vec{W} = -mg \begin{bmatrix} -\mathrm{s}(\alpha_y) \\ \mathrm{c}(\alpha_y)\mathrm{s}(\alpha_x) \\ \mathrm{c}(\alpha_y)\mathrm{c}(\alpha_x) \end{bmatrix}_{R_t}. \tag{1}$$

The force balance is assumed to be a one degree-of-freedom system, so its dynamical behavior is described along $\vec{z}_t$. The repulsive diamagnetic forces are perpendicular to $\vec{z}_t$ and are therefore neglected. The electromagnetic force $\vec{F}_{elec}$ produced by the two coils is defined as:

$$\vec{F}_{elec} = \mathrm{I}(\gamma z + \beta)\vec{z}_t, \text{ with } \mathrm{I} = i_0 + i. \tag{2}$$

The current I corresponds to the numerical command sent to the controller, with i_0 being the known constant command producing the electromagnetic force that ensures the levitation, and i the command that controls the height of the indenter. The constant parameters γ and β are studied in the following section. In this modeling, the force $\vec{F}_c$ applied by the cantilever on the indenter is assumed to be aligned with the motion of the micromanipulator, and is therefore defined as:

$$\vec{F}_c = -\Delta z K_c \vec{z}_t, \tag{3}$$

with $\Delta z = z - z_{\mathrm{PI}}$, z_{PI} being the position of the PI micromanipulator, and K_c the unknown stiffness to be estimated. Finally, the dynamical behavior of the indenter is described by the following model:

$$\begin{aligned} m\ddot{z} + K_v\dot{z} - i_0\gamma z =& i(\gamma z + \beta) + i_0\beta - mg\mathrm{c}(\alpha_x)\mathrm{c}(\alpha_y) \\ & - \Delta z K_c \end{aligned} \tag{4}$$

in which K_v models the air friction force $\vec{F}_v$.

B. Parameter identification

The mass m of the indenter is equal to 4.5 ± 0.1 mg and the offset current i_0 is set to 130 mA. Considering the static equilibrium of indenter in levitation, i.e. without table tilt, inertial forces or cantilever effort, and with $i = 0$, the previous mechanical model (4) leads to:

$$\beta = \frac{mg}{i_0} = 3.396 \times 10^{-4} \text{ N.A}^{-1}. \tag{5}$$

Then, parameters K_v and γ are estimated using the free response of the indenter around its equilibrium position. Fig. 2 shows both the measured displacement of the indenter, and the fitted output of a linear model of the form:

$$\ddot{z} + a_1\dot{z} + a_0 z = 0, \text{ with } a_0 = 737.466 \text{ and } a_1 = 0.389. \tag{6}$$

Using (4), the coefficients a_0 and a_1 are expressed as:

$$a_0 = \frac{-i_0\gamma}{m}, \; a_1 = \frac{K_v}{m} \tag{7}$$

and give $\gamma = -0.026$ kg.s^{-2}.A^{-1} and $K_v = 1.749 \times 10^{-6}$ kg.s^{-1}.

III. Equivalent State-Space Representation

The first step of the methodology consists in determining an exact representation of the true behavior of the force balance, considering all the external disturbances and unmodeled dynamics. The theorem of equivalent representation

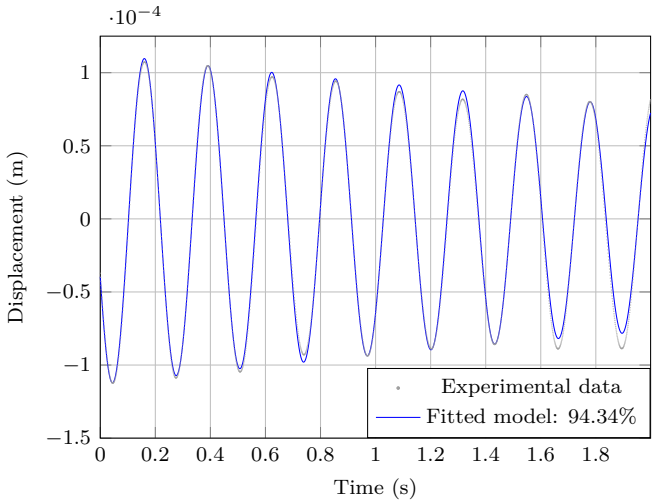

Fig. 2. Free response of the indenter: comparison between the measured displacement and the fitted model.

given in [7] is based on an identified linear model ($\mathcal{M}$) of order $p > 0$, defined by the companion matrices A, B, C, respectively the state, input and output matrices of ($\mathcal{M}$) with appropriate dimensions.

Theorem 1 (Equivalent representation): For any given nonlinear system ($\mathcal{S}$) and linear model ($\mathcal{M}$), it exists a virtual input $\mathcal{I}(t)$ such that the nonlinear dynamics of the input-output signals $(u(t), y(t))$ of ($\mathcal{S}$) can be equivalently represented by the following linear state-space equations:

$$(\mathcal{S}) \Leftrightarrow \begin{cases} \dot{X} = AX + B(u + \mathcal{I}), \\ y = CX \end{cases} \tag{8}$$

in which $X \in \mathbb{R}^p$ is the state vector of the equivalent model with the following components:

$$X = \begin{bmatrix} y & \dot{y} & \dots & y^{(p-1)} \end{bmatrix}^T. \tag{9}$$

The virtual input is therefore additive on the control input channel and depicts the discrepancy of the linear model ($\mathcal{M}$). This means that external disturbances, modeling errors such as nonlinearities and remaining unknown dynamics are included in $\mathcal{I}$, so that the actual output of the physical system under study is equivalently reproduced. The evolution matrix A of the model ($\mathcal{M}$) chosen for the force balance is determined based on the previously identified free response of the indenter. The current i is considered as the input signal of the force balance. According to (2), the electromagnetic force generated by I depends on the constant parameters γ and β, but also on the displacement of the indenter. Based on (4), a constant static gain is determined for ($\mathcal{M}$) neglecting the dependence on z, resulting in a control matrix B given by:

$$B = \begin{bmatrix} 0 \\ \frac{\beta}{m} \end{bmatrix}. \tag{10}$$

Considering $X = \begin{bmatrix} z & \dot{z} \end{bmatrix}^T$ as the state vector of the force balance, the equivalent state-space representation of its dynamics is therefore expressed as follows:

$$(\mathcal{S}) \Leftrightarrow \begin{cases} \dot{X} = \begin{bmatrix} 0 & 1 \\ -737.466 & -0.389 \end{bmatrix} X + \begin{bmatrix} 0 \\ 75.436 \end{bmatrix} (i + \mathcal{I}), \\ z = \begin{bmatrix} 1 & 0 \end{bmatrix} X. \end{cases} \tag{11}$$

IV. Estimation of the virtual input

Once the equivalent model of the indenter has been determined, an estimate of the virtual input $\mathcal{I}$ is required to apply the proposed method. Indeed, the dynamics of the force applied by the cantilever on the indenter is not described by the identified model ($\mathcal{M}$) and is therefore included in $\mathcal{I}$. In control theory, the virtual input $\mathcal{I}$ corresponds to an unknown input that can be estimated using various techniques. As in Reference [7], a Linear Kalman Filter is turned into an Extended State observer (ES-LKF) which is a common technique for estimating unknown external disturbances and unmodeled dynamics. In such an observer design, all unknown inputs are lumped into an additional state to be estimated with the initial state vector X. The extended state vector $X^e \in \mathbb{R}^3$ is thus defined as:

$$X^e = \begin{bmatrix} z & \dot{z} & \mathcal{I} \end{bmatrix}^T \tag{12}$$

and leads to the following extended state-space representation:

$$\begin{cases} \dot{X}^e = \mathcal{A}X^e + \mathcal{B}i + \mathcal{D}\dot{\mathcal{I}}, \\ z = \mathcal{C}X^e \end{cases} \tag{13}$$

in which

$$\mathcal{A} = \begin{bmatrix} 0 & 1 & 0 \\ -737.466 & -0.389 & 75.436 \\ 0 & 0 & 0 \end{bmatrix}, \mathcal{B} = \begin{bmatrix} 0 \\ 75.462 \\ 0 \end{bmatrix}, \\ \mathcal{D} = \begin{bmatrix} 0 & 0 & 1 \end{bmatrix}^T, \ \mathcal{C} = \begin{bmatrix} 1 & 0 & 0 \end{bmatrix}. \tag{14}$$

According to the principle of equivalent representation, no uncertainty is introduced by the known matrices of ($\mathcal{M}$), the discrepancy of the model only lies in the virtual input $\mathcal{I}$. However, the consistency of the estimated virtual input $\hat{\mathcal{I}}$ depends on the reliability of the ES-LKF inputs. Indeed, if the signals given to the observer are different from the input-output signals of ($\mathcal{S}$), the virtual input $\mathcal{I}$ may not be estimated correctly. Therefore, the observer must take into account the uncertainty associated with its inputs to ensure the potential metrological traceability of the approach. The input signals of the ES-LKF are the varying current i and the displacement z of the indenter measured with noise. White Gaussian stochastic processes ω and ω_i with zero mean and infinite variance are used to model respectively the unknown dynamics of the virtual input [7] and the noise of the output current of the power supply:

$$\begin{cases} \dot{\mathcal{I}} = \omega, \\ i = i^{\mathrm{c}} + \omega_i, \end{cases} \tag{15}$$

with i^{c} the known numerical value of i. The extended state-space representation (13) is therefore turned into the

following stochastic model:

$$\begin{cases} \dot{X}^e = \mathcal{A}X^e + \mathcal{B}i^{\mathrm{c}} + \delta\Omega, \\ z = \mathcal{C}X^e. \end{cases} \tag{16}$$

with $\delta = \begin{bmatrix} \mathcal{B} & \mathcal{D} \end{bmatrix} \in \mathbb{R}^{3\times 2}$, $\Omega = \begin{bmatrix} \omega_i & \omega \end{bmatrix}^T \in \mathbb{R}^2$. The continuous model (16) is discretized using a zero-order hold operating at T_s. Considering z_k as the discrete displacement of the indenter measured with a discrete-time band-limited white Gaussian noise v_k with zero mean and variance $R \in \mathbb{R}$, the discrete stochastic evolution of X_k^e and z_k are described by:

$$\begin{cases} X_{k+1}^e = \mathcal{F}X_k^e + \mathcal{G}i_k^{\mathrm{c}} + \Omega_k, \\ z_k = \mathcal{C}X_k^e + v_k, \end{cases} \tag{17}$$
$$\mathcal{F} = e^{\mathcal{A}T_s},\ \mathcal{G} = \int_0^{T_s} e^{\mathcal{A}t}\mathcal{B}dt$$

in which Ω_k is a band-limited white Gaussian process noise with a zero-mean and a covariance matrix Q given by:

$$Q = E\left[\Omega_k\ \Omega_k^T\right] = \int_0^{T_s} e^{\mathcal{A}t}\delta W \delta^T e^{\mathcal{A}^T t}dt, \tag{18}$$
$$\text{with}: W = \begin{bmatrix} w_{\mathrm{PSD}i} & 0 \\ 0 & w_{\mathrm{PSD}} \end{bmatrix},$$

w_{PSD} and $w_{\mathrm{PSD}i}$ being respectively the constant power spectral densities of the stochastic process noise ω and ω_i, set to 1×10^{-4} A^2/Hz and 1.1095×10^{-12} A^2/Hz. Let $\hat{X}_0^e$ and P_0 be initial conditions, the prediction-update steps of the Kalman filter are given by the following equations:

$$\begin{aligned} &\hat{X}_{k|k-1}^e = \mathcal{F}\hat{X}_{k-1}^e + \mathcal{G}i_{k-1}^{\mathrm{c}}, \\ &P_{k|k-1} = \mathcal{F}P_{k-1}\mathcal{F}^T + Q, \\ &K_k = P_{k|k-1}\mathcal{C}^T(\mathcal{C}P_{k|k-1}\mathcal{C}^T + R)^{-1}, \\ &\hat{X}_k^e = \hat{X}_{k|k-1}^e + K_k(z_k^m - \mathcal{C}\hat{X}_{k|k-1}^e), \\ &P_k = (I_3 - K_k\mathcal{C})P_{k|k-1} \end{aligned} \tag{19}$$

in which z_k^m is the actual displacement value measured at time t_k. The estimated virtual input $\hat{\mathcal{I}}$ corresponds to the third component of $\hat{X}_k^e$, the third diagonal component of $\hat{P}_k$ gives the variance σ_k^2 of the related observation error. An interval $\left[\hat{\mathcal{I}}_k\right]$ that must include $\mathcal{I}$ is determined at the k-th time instant as follows:

$$\left[\hat{\mathcal{I}}_k\right] \triangleq \left[\hat{\mathcal{I}}_k - 3\sigma_k,\ \hat{\mathcal{I}}_k + 3\sigma_k\right]. \tag{20}$$

Fig. 3 shows the estimate of the virtual input $\hat{\mathcal{I}}$ along with the 3σ bounds, whose dynamics is related to the action of the free end of the cantilever on the controlled position of the indenter. The displacement z_{PI} of the PI micromanipulator moving the cantilever is shown in Fig. 4.

V. Virtual Input Shaping

The virtual input $\mathcal{I}$ corresponds to the discrepancy of $(\mathcal{M})$ and thus represents the dynamics of various unknown quantities. Therefore, the force applied by the cantilever on the indenter must be distinguished from the rest in order to estimate its stiffness K_c. To do so, a shaping model h is

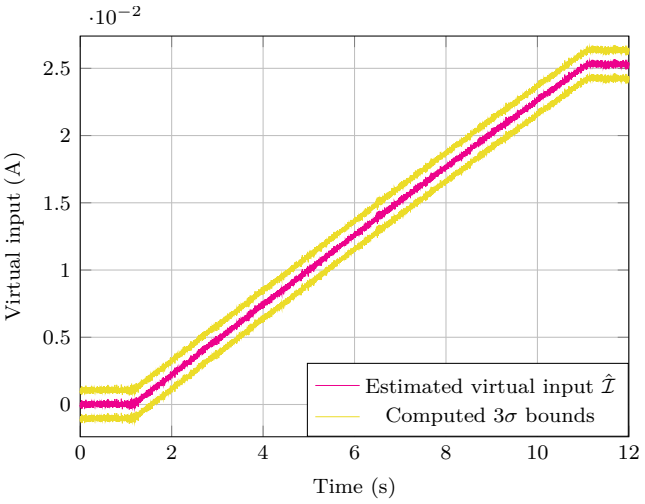

Fig. 3. Plot of the estimated virtual input $\hat{\mathcal{I}}$ with the 3σ bounds.

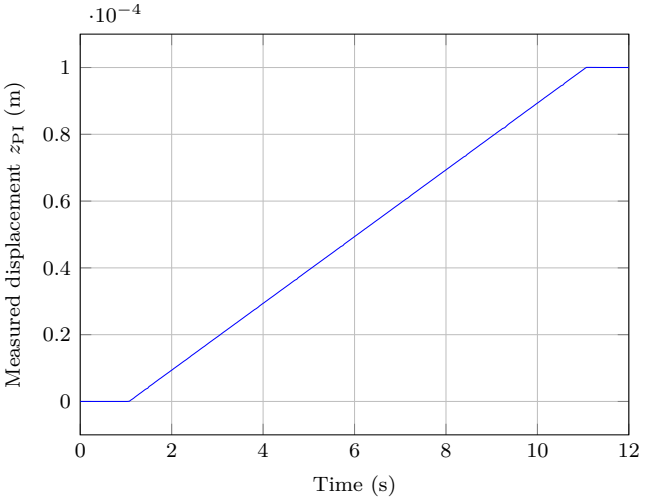

Fig. 4. Plot of the PI micromanipulator displacement z_{PI}.

introduced to describe the dynamics of the virtual input $\mathcal{I}$ as follows:

$$\mathcal{I}(t) = h(Q(t), D(t)) + \varepsilon(t), \tag{21}$$

with Q and D two vectors that respectively gathers the quantities to be estimated and measurement biases. More precisely, D refers to significant inputs which can be measured or estimated, likely to deteriorate the estimation of Q if they are not taken into account. The Residual Shaping Error (RSE) ε stems from the principle of equivalent representation, and corresponds to unknown remaining dynamics. The mechanical model (4) is equal to:

$$\begin{aligned} \ddot{z} + \frac{K_v}{m}\dot{z} - \frac{i_0\gamma}{m}z =& \frac{\beta}{m}i + i\frac{\gamma}{m}z + g\left[1 - \mathrm{c}(\alpha_x)\mathrm{c}(\alpha_y)\right] \\ &- \frac{z - z_{\mathrm{PI}}}{m}K_c, \end{aligned} \tag{22}$$

and reveals the expression of the identified model $(\mathcal{M})$. During a test, the tilt of the table is modified by slowly

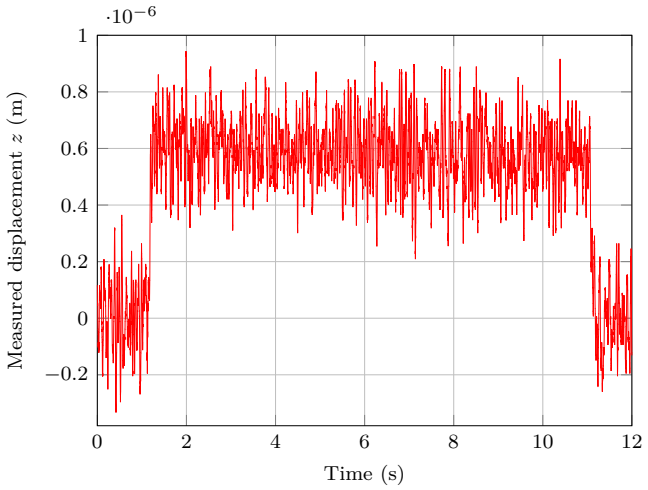

Fig. 5. Measurement of the indenter position z during loading phase with closed-loop control.

varying angles α_x, α_y, which disturbs the balance of forces and thus deteriorates the estimate of stiffness K_c. The offset current i_0 and the displacement z_{PI} of the cantilever to be tested are considered as external inputs with respect to $(\mathcal{S})$. Therefore, the vectors Q and D are defined as follows:

$$Q = K_c \ , \ D = \begin{bmatrix} i_0 & \alpha_x & \alpha_y & z_{\text{PI}} \end{bmatrix}^T . \tag{23}$$

Hence, the virtual input shaping considered in this paper is expressed by:

$$\mathcal{I} = \frac{i_0\gamma}{mg} iz + i_0\Big[1 - \text{c}(\alpha_x)\text{c}(\alpha_y)\Big] - \frac{i_0 \Delta z}{mg} K_c + \varepsilon. \tag{24}$$

In this manner, the dynamics of the force balance is described by the following equivalent model:

$$\ddot{z} + \frac{K_v}{m}\dot{z} - \frac{i_0\gamma}{m} z = \frac{\beta}{m}\Big(i + \mathcal{I}\Big). \tag{25}$$

VI. Uncertainty propagation

The observation error related to the estimated virtual input $\hat{\mathcal{I}}$ is propagated towards the quantities of interest in Q thanks to the shaping model (24). The calculation is addressed using the framework of interval analysis [8], taking into account the possible uncertain parameters involved.

A. Interval analysis : useful concepts

A real interval $[x]$ is a closed subset of $\mathbb{R}$:

$$[x] = [x^-, x^+] = \{x \in \mathbb{R} \mid x^- \leq x \leq x^+\}, \tag{26}$$

with x^- and x^+ respectively the lower and upper bounds of $[x]$. The set of real intervals is denoted by $\mathbb{IR}$. A box $[\mathbf{x}]$, also a real interval vector, is defined as the Cartesian product of n real intervals:

$$[\mathbf{x}] = [x_1^-, x_1^+] \times \ldots \times [x_n^-, x_n^+] = [x_1] \times \ldots \times [x_n] \in \mathbb{IR}^n. \tag{27}$$

The lower and upper bounds of a box $[\mathbf{x}]$ corresponds respectively to $\mathbf{x}^- = (x_1^-, \ldots, x_n^-)^T$ and $\mathbf{x}^+ = (x_1^+, \ldots, x_n^+)^T$. Arithmetic operations $\circ \in \{+, -, \ . \ , /\}$ between real numbers have been extended to the framework of intervals following the form given in [8]. A contractor $\mathcal{C}$ is an operator able to reduce a box $[\mathbf{x}] \in \mathbb{IR}^x$ by removing parts that do not satisfy an expression of the form $\mathbf{f}(\mathbf{x}) \in [\mathbf{y}]$, with $\mathbf{f}$ a function from $\mathbb{R}^x$ to $\mathbb{R}^y$, and $[\mathbf{y}]$ a box of $\mathbb{IR}^y$. This membership relation corresponds to a constraint, and is associated with the set $\mathbb{S} = \{\mathbf{x} \in \mathbb{R}^x \mid \mathbf{f}(\mathbf{x}) \in [\mathbf{y}]\}$. Hence, the contraction of a given box $[\mathbf{x}]$ under this constraint returns a box $\mathcal{C}([\mathbf{x}]) \subset [\mathbf{x}]$ that satisfies $\mathcal{C}([\mathbf{x}]) \cap \mathbb{S} = [\mathbf{x}] \cap \mathbb{S}$.

TABLE I
Numerical values used for uncertainty propagation

Parameter	Scalar value	Interval
i_0 (A)	0.130	-
γ (kg.s^{-2}.A^{-1})	-0.026	-
m (kg)	-	$[4.4 \times 10^{-6},\ 4.6 \times 10^{-6}]$
g (m.s^{-2})	9.807	-

B. Stiffness estimation

The interval $[K_c]$ is introduced for the stiffness to be estimated. In the same way, the measurement bias vector D is replaced with the following box $[\mathbf{d}^m]$:

$$[\mathbf{d}^m] = [i_0] \times [\alpha_x] \times [\alpha_y] \times [z_{\text{PI}}] \in \mathbb{IR}^4, \tag{28}$$

$[i_0]$ being a degenerate interval, i.e. it only contains the known scalar value i_0. The tilt angles α_x and α_y have been estimated a priori for this paper and are thus considered bounded as follows:

$$\begin{aligned} [\alpha_x] &= [-1.75 \times 10^{-10} \text{ rad},\ 1.75 \times 10^{-10} \text{ rad}], \\ [\alpha_y] &= [-2.62 \times 10^{-10} \text{ rad},\ 2.62 \times 10^{-10} \text{ rad}]. \end{aligned} \tag{29}$$

The displacement z_{PI} is provided in real-time by the PI-controller with a precision of ± 2 μm. An interval $[z_{\text{PI}}]$ is defined as $[z_{\text{PI}} - 2 \times 10^{-6}\ \text{m},\ z_{\text{PI}} + 2 \times 10^{-6}\ \text{m}]$ to carry out the calculation. In the same way, $[z] = [z - 3\sqrt{R}\ \text{m},\ z + 3\sqrt{R}\ \text{m}]$ and $[\text{I}] = [\text{I} - 3\sigma\ \text{A},\ \text{I} + 3\sigma\ \text{A}]$ are introduced, with $\sigma = 3.505 \times 10^{-4}$ A. Considering $\mathbf{d}$ as an element of $[\mathbf{d}^m]$, the possible values of the cantilever stiffness are therefore described by the solution set $\mathbb{S}_k$ defined as:

$$\mathbb{S}_k = \Big\{K_c \in [K_c]_0 \mid \exists\ \mathbf{d} \in [\mathbf{d}^m],\ h(K_c, \mathbf{d}) \in [\hat{\mathcal{I}}_k]\Big\}, \tag{30}$$

with $[K_c]_0 = [-0.4\ \text{N.m}^{-1},\ 0.4\ \text{N.m}^{-1}]$ the initial search space. The membership relation $h(Q, \mathbf{d}) \in [\hat{\mathcal{I}}_k]$ is considered as a constraint and is thus used to contract $[K_c]_0$. The forward-backward contractor is implemented to compute the unknown stiffness of the cantilever. A sequence of primitive constraints is determined from the shaping model and is evaluated forward and backward. Further information on its operation can be found in [9]. Represented as a graph, the primitive decomposition of the virtual input shaping is said to be acyclic with respect to K_c, which guarantees that the contraction is minimal. The numerical value of the variables included in (24) are summarized in Table I. Fig. 5 shows the position of the indenter in closed-loop with its equilibrium

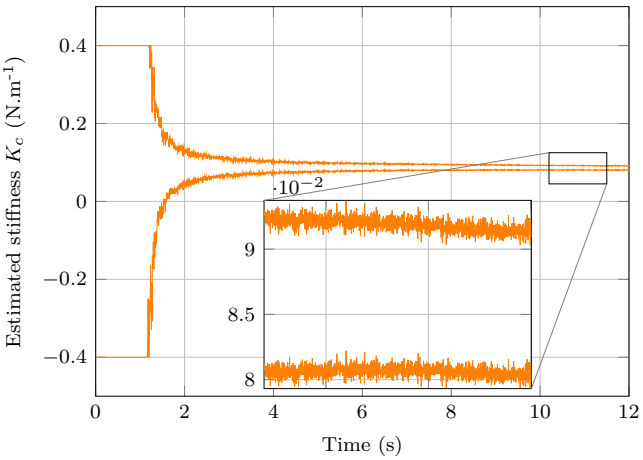

Fig. 6. Plot of the post-computed solution sets $\mathbb{S}_k$

altitude taken as a reference, regulated using an integral-derivative controller operating at $f_s = {}^1/_{T_s} = 1$ kHz. During the loading phase by the PI micromanipulator, a steady-state error on the indenter position remains due to the constant loading velocity. Fig. 6 shows the estimated bounds of $\mathbb{S}_k$ with respect to time, narrowing as z_{PI} increases. As the stiffness of the cantilever is assumed to be constant over the trial duration, the final estimated interval $[K_c]$ is defined as:

$$[K_c] = \bigcap_{k=0}^{12 f_s} \mathbb{S}_k, \text{ and thus equals } [0.082 \text{ N.m}^{-1},\ 0.090 \text{ N.m}^{-1}]. \tag{31}$$

VII. Discussion

The intersection of the computed solution sets is used to determine the final interval $[K_c]$. In this work, the computed bounds seem to converge towards constant values, which is consistent as a constant parameter is estimated. However, the calculation is based on the assumption that $\varepsilon = 0$ which is not necessarily true. Indeed, if disturbances with significant dynamics have been omitted in the shaping of the virtual input, the computed sets $\mathbb{S}_k$ may be disjoints and thus lead to $[K_c] = \emptyset$. In this case, an additional indicator is needed to reject estimated sets that have been distorted, or the shaping must be refined to take these disturbances into account. The table on which the electromagnetic force balance is mounted presents a residual inertial regime due to an imperfect vibration isolation system. As a consequence, the finished electromagnetic force balance will include a dedicated triaxial accelerometer to measure the disturbing inertial forces in real-time. Further in-depth studies will also examine the importance of the contact point location in the stiffness estimation process.

VIII. Conclusion

This work highlights the suitability of the equivalent representation paradigm mentioned earlier in the introduction, for estimating unknown quantities and their related uncertainty. The methodological proposal is illustrated on a force balance dedicated to the estimation of the unknown stiffness of a flexible cantilever. According to the theorem of equivalent representation, the dynamical behavior of the force balance is perfectly described by an identified linear model ($\mathcal{M}$) thanks to a virtual input $\mathcal{I}$, which corresponds to the discrepancy of ($\mathcal{M}$). A linear Kalman filter is used as an ESO to compute an estimated interval $[\hat{\mathcal{I}}]$ based on the filter observation error, and meant to enclose the theoretical value of $\mathcal{I}$. A shaping model is then introduced to describe the dynamics of the virtual input depending on the quantities to be estimated and measurement biases. The virtual input shaping model is finally used to propagate the estimated interval $[\hat{\mathcal{I}}]$ towards the quantities of interest. The uncertainty propagation is carried out within the framework of interval analysis, using the forward-backward contractor. In the future, mechanical characterization activities will be undertaken with the French NMI in the field of small forces, enabling the proposed approach to be compared with metrological means.

Acknowledgment

This work has been funded by the french National Research Agency (ANR) under the project ANR-23-CE42-0022-01. This work has been supported by the EIPHI Graduate school (contract "ANR-17-EURE-0002") and by the Bourgogne-Franche-Comté Region. This work was partly supported by the french RENATECH network and its FEMTO-ST technological facility. The authors would also like to thank the facilities of the MIFHySTO platform, as well as the French ROBOTEX network and its FEMTO-ST technological facility funded under Grant ANR-10-EQPX-44-01.

References

[1] R. Kohli and K. Mittal, "Developments in surface contamination and cleaning." Oxford: William Andrew Publishing, 2012, pp. 215–306.
[2] G. A. Shaw, "Current state of the art in small mass and force metrology within the international system of units," *Measurement Science and Technology*, vol. 29, no. 7, p. 072001, may 2018.
[3] F. Amokrane, A. Drouot, J. Abadie, and E. Piat, "Nanoforce estimation using interval observer: Application to force sensor based on diamagnetic levitation," in *2021 World Congress (IFAC 2021)*, vol. 53, no. 2, Tokyo, Japan, sep 2020, pp. 8638 – 8643.
[4] J. Pratt, J. Kramar, D. Newell, and D. Smith, "Review of si traceable force metrology for instrumented indentation and atomic force microscopy," *Measurement Science and Technology*, vol. 16, p. 2129, 09 2005.
[5] S. Eichstädt, V. Wilkens, A. Dienstfrey, P. Hale, B. Hughes, and C. Jarvis, "On challenges in the uncertainty evaluation for time-dependent measurements," *Metrologia*, vol. 53, no. 4, p. S125, jun 2016.
[6] S. Eichstädt, K. Ruhm, and A. Shestakov, "Dynamic measurement and its relation to metrology, mathematical theory and signal processing: a review," *Journal of Physics: Conference Series*, vol. 1065, p. 212018, 08 2018.
[7] F. Amokrane, E. Piat, J. Abadie, A. Drouot, and J. A. Escareno, "State Observation of a Specific Class of Unknown Nonlinear SISO Systems using Linear Kalman Filtering," in *Conference on Decision and Control*, Nice, France, Dec. 2019.
[8] R. E. Moore, R. B. Kearfott, and M. J. Cloud, *Introduction to Interval Analysis*. Society for Industrial and Applied Mathematics, 2009.
[9] F. Benhamou, F. Goualard, L. Granvilliers, and J.-F. Puget, "Revising hull and box consistency." 01 1999, pp. 230–244.